PH DEPENDENCE OF IRON SPECIATION IN *SACCHAROMYCES CEREVISIAE* VACUOLES

An Undergraduate Research Scholars Thesis

by

JOEL P FERRER

Submitted to the Undergraduate Research Scholars program at
Texas A&M University
in partial fulfillment of the requirements for the designation as an

UNDERGRADUATE RESEARCH SCHOLAR

Approved by Research Advisor: Dr. Paul A. Lindahl

May 2017

Major: Biomedical Sciences

TABLE OF CONTENTS

ABSTRACT

pH Dependence of Iron Speciation in *Saccharomyces cerevisiae* Vacuoles

Joel P Ferrer
Department of Biomedical Sciences
Texas A&M University

Research Advisor: Dr. Paul A. Lindahl
Department of Chemistry
Texas A&M University

Vacuoles in yeast are vital organelles that take on many important biological roles. They are responsible for collecting and detoxifying iron such that reactive oxygen species are not formed. They are also important storage organelles for many nutrients including iron. In fact, if enough iron is stored within the yeast vacuole, the cell is able to survive in iron deficient conditions. A model for iron trafficking in the vacuole has been proposed previously by Cockrell *et al.* which suggests that iron is imported as iron (II) where, once inside, it is oxidized to iron (III). Under standard conditions, it is known that yeast vacuoles tend to be more acidic, around pH 5, due to a proton pump encoded with many subunits one of them being VMA2. Because the molecule to which the iron is ligated with is based largely on the vacuolar pH, it is suspected that when the subunit corresponding to VMA2 is knocked out *in vivo*, the iron will favor nanoparticles rather than its polyphosphate ligand. Previously, it has been shown *in vitro* that this interconversion is possible however *in vivo* studies have not been conducted. In addition to the interconversion, it was hypothesized that, if the pH of the growth medium is lowered below pH 5, the acidic conditions will be able to "rescue" the cell from the perils of alkalinity. These hypothesizes were tested by growing *Saccharomyces cerevisiae* cells with a BY4741 background

with and without the VMA2 subunit. The cells were then harvested and analyzed using a combination of biophysical techniques including Mössbauer spectroscopy, and electron paramagnetic resonance (EPR). As a result, it was seen that, indeed, this interconversion was possible *in vivo*. Moreover, when the subunit of the vacuolar ATP-ase was knocked out, there was a sizable increase in total cellular iron which suggests that extracellular pH of the growth medium affects the mitochondria resulting in a dysregulation in iron import.

ACKNOWLEDGEMENTS

I would like to thank everyone that has guided me and given me perspective in not only my research but my life. To Nate, Mike, Trang, Josh, and Cody, I could not have done it without you guys. Our constant laughs and deep conversations kept me sane and you all are incredible people and scientists. I want to thank Dr. Lindahl for being an exceptional mentor and keeping me excited about research even through the troubling times. The Lindahl lab has truly been a blessing and I can't thank any of you enough.

Finally, I would like to thank my parents and family from the bottom of my heart. You all inspire me every day to keep going and to continue pushing myself to be better. Without your love and support, I can't even begin to imagine where I would be. You all have shaped the man I have become and, for that, I am eternally grateful. I love you all to the moon and back.

NOMENCLATURE

Fe	Iron
OD_{600}	Optimal density at 600 nm
DD	Distilled, Deionized
DI	Deionized
MB	Mössbauer
Fe–S	Iron–sulfur

CHAPTER I

INTRODUCTION

Iron (Fe) is a vital cellular nutrient that, when paired with sulfur as iron-sulfur clusters (ISCs), acts as an important cofactor in oxidative phosphorylation.[1] Iron is imported into the cell via iron transporters including the Ftr1/Fet3 complex, Fet4, and Smf1.[2] Once imported, the Fe is shuttled to the mitochondria and used to generate ISCs or to the vacuole for storage. Though studied less than mitochondrial iron, vacuoles are the central character in many physiological functions. These functions include sequestering Fe from the cytosol[3] and detoxifying it such that the formation of reactive oxygen species (ROS) is limited as these products are detrimental to cellular DNA, lipids, and proteins.[4] Moreover, storage of Fe in the vacuoles allows for the cell to live and replicate for many generations even in iron limiting conditions.[5]

One of the most important physiological factors of the vacuole is their acidity. Brett and coworkers has shown experimentally that the pH statistic for wild-type *Saccharomyces cerevisiae* vacuoles ranges from 4.8 to 5.5.[6] This acidic property is controlled by a vacuolar H^+-ATPase (V-ATPase) which is composed of two domains, V_0 and V_1. When either of these subunits are disturbed, the V-ATPase loses its function as a proton pump and, as such, the vacuole loses its acidic property. In this study, the V-ATPase is perturbed by knocking out the β-subunit of the V_1 domain in *Saccharomyces cerevisiae*.

The vacuolar biochemistry of V-ATPase has been studied extensively by Kane and coworkers and they have derived many important conclusions. Diab *et al.* demonstrated that in

Vma2 mutants there is a clear upregulation of the "iron regulon" genes including the mitochondrial protein, Aft1p.[7,8] This reported upregulation resulted in an approximate 20% increase of total cellular Fe in the Vma2 mutant compared to wild-type. However, the Fe ligand environment was not provided.

In contrast, previous work performed by Cockrell *et al* provides a possible ligand environment for vacuolar iron under normal vacuolar conditions in wild-type *Saccharomyces cerevisiae*. Cockrell and coworkers suggest that once Fe is imported into the vacuole as Fe^{II}, it is then oxidized to Fe^{III} where it then ligates with polyphosphate. Moreover, in an *in vitro* study varying only pH, they were able to demonstrate that it is indeed possible for Fe^{III}-polyphosphate to interconvert to Fe^{III}-nanoparticles.[9]

The study presented here is focused on explaining the effects of varying pH of the growth medium using Vma2 mutants with a BY4741 background as well as wild-type BY4741. The data below depicts a trend which suggests that as pH of the growth medium increases, rather existing as Fe^{III}, we see a shift in cellular equilibrium towards Fe^{III} nanoparticles. We demonstrate that in these Vma2 mutants, the "iron regulon" is upregulated more than 20% in contrast to wild-type and propose a mechanism involving dysfunctional mitochondria due to high pH to explain this phenomenon.

CHAPTER II

EXPERIMENTAL PROCEDURES

TABLE 1

Yeast strains used in this study.

STRAIN	GENOTYPE	SOURCE
BY4741	*MATa his3Δ1 leu2Δ0 met15Δ0 ura3Δ0*	Patricia Kane
BY4741 *vma2Δ*	*MATa his3Δ1 leu2Δ0 met15Δ0 ura3Δ0 vma2Δ*::*kanMX*	Patricia Kane

Yeast Strains and Growth

The strains used throughout this study are listed above in Table 1. They were grown in YPAD (1% yeast extract, 2% peptone, 2% dextrose, 0.01% adenine) or supplemented minimal medium (0.17% YNB, 0.5% $(NH_4)_2SO_4$, 2% dextrose including all supplements indicated above). The mentioned mediums were both buffered with 50 mM sodium succinate hexahydrate to varying pH ranges of pH 3 – 7. The cells were grown from glycerol stocks that were prepared by growing cells for 3 days on agar plates containing the YPAD medium described above. Following this growth, the cells were washed off the plate and resuspended in 15% glycerol to be stored at –80 °C.

Once ready, cells were scraped from the frozen glycerol stock onto an agar plate. After growing, a single colony was then inoculated into 50 mL culture flasks of supplemented minimal medium until $OD_{600} \approx 0.80$. The 50 mL culture flask was then inoculated into 1 L of the same medium and allowed to grow until the $OD_{600} \approx 0.80$.

Instrumentation

Mössbauer (MB) samples were prepared by centrifuging whole cells at 5000g six times (Sorvall Evolution RC centrifuge, SLC-6000 rotor). For the first three washes, cells were washed and resuspended in 100 mL of 1 mM EDTA adjusted to pH 7.4. For the final three washes, cells were resuspended and washed in DD water and, after the third DD water wash, the cells were resuspended once more. They were then spun down into a MB cup using a microcentrifuge (Beckman Coulter Optima L-90K ultracentrifuge, SW-32 Ti rotor) for 5 minutes at 5000g and immediately frozen in liquid N_2 for MB analysis. All MB samples were analyzed at a temperature of 5 K.

EPR samples were prepared using a similar methodology as described above. Whole cell samples were centrifuged at 5000g three times in 1 mM EDTA and another three times in DD water. Following this, the washed cells were centrifuged into an EPR tube (Beckman Coulter Avanti J-26 XP, JS-5.3 rotor) for 5 minutes at 3000g where the EPR sample was immediately frozen in liquid N_2 for EPR analysis. All EPR samples were analyzed at 30 dB at a temperature of 5 K.

CHAPTER III

RESULTS

Mössbauer Spectra Analysis

MB analysis of whole cell samples of BY4741 grown at pH 3, pH 5, pH 6, and pH 7 (Figure 1a), we see a very clear trend. As the pH of the growth medium is increased, there is a notable decrease in nonheme high-spin Fe^{III}. The spectra of pH 3 shows that 52% of the total cellular iron is NNHS Fe^{III} (Figure 1b), which is associated to vacuolar iron. As pH is increased to 5, NHHS Fe^{III} is decreased to 36% of the total, pH 6 is decreased to 18%. However, in the final sample of the wild type at pH 7, the percentage of NHHS Fe^{III} increases to just over 41% likely due to a slightly higher OD_{600} at time of cell harvest. In addition to the loss of NHHS Fe^{III}, it is significant to note that as pH increases, the total cellular Fe concentration decreases.

Similarly, we see this same trend in the mutant ΔVMA2 cells grown with varying pH (Figure 2a). However, the important difference to make note of is how the total cellular iron does not diminish as the WT strain does. We suggest that, unlike how the WT strain appears to lose its ability to import iron, the mutant strain is actively converting the NHHS Fe^{III} to Fe^{III} oxyhydroxide nanoparticles. This is supported by the breakdown of the mutant strain's MB spectra (Figure 2b). The NHHS Fe^{III} is shown to be approximately 44% of the total cellular iron while the nanoparticles make up about 10%. In contrast, when looking at the MB spectra for the mutant strain at pH 7, there is a dramatic shift from NHHS Fe^{III} to nanoparticles resulting in less than one percent of the spectra being NHHS Fe^{III} while nanoparticles consume the total cellular iron at 58%. In addition to this shift, there is also the development of a NHHS Fe^{II} feature. This

intensity of this feature also seems to increase in intensity as the pH of the growth medium increases.

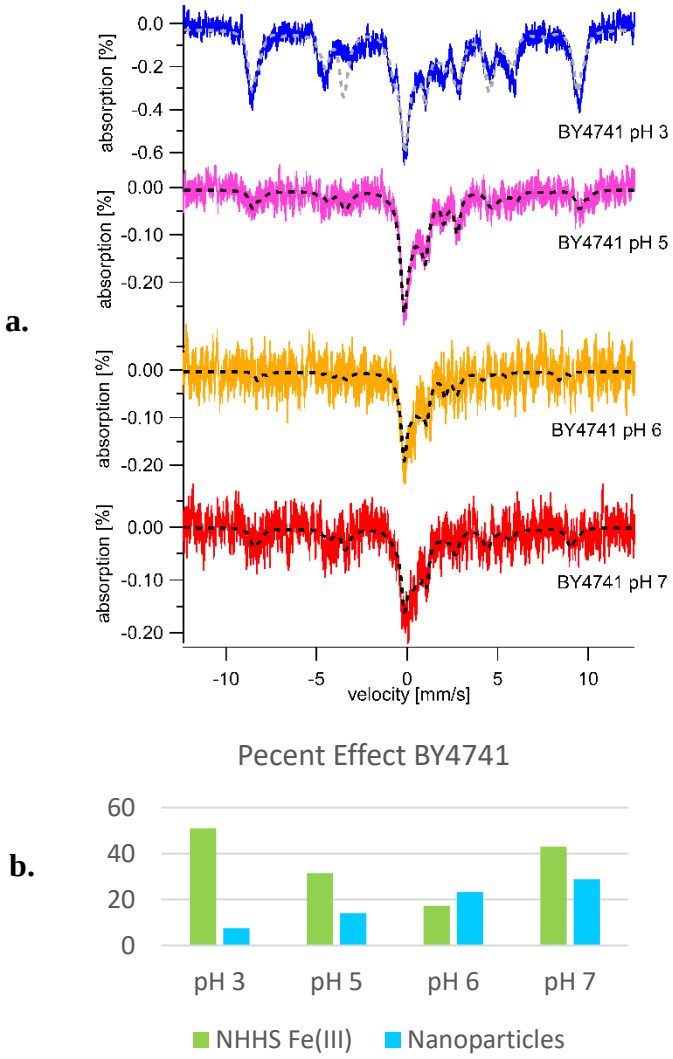

FIGURE 1: a.) The BY4741 WT strain grown at various pH; spectra were collected at 5 K and harvested at $OD_{600} \approx 0.8$. b.) Bar chart relating the changes in percent effect between NHHS Fe^{III} and nanoparticles of the WT strain.

a.

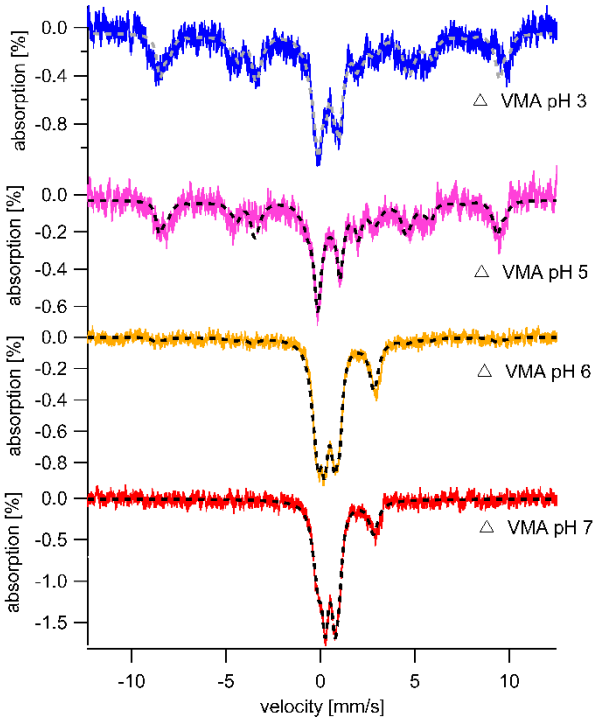

b.

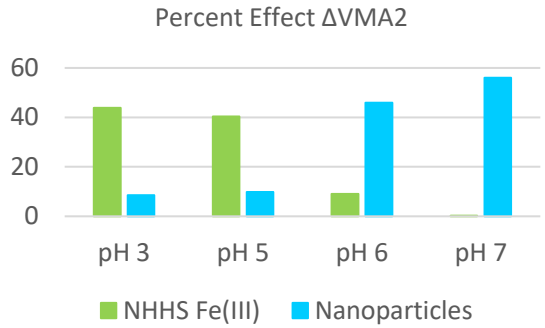

FIGURE 2: a.) The ΔVMA2 mutant strain grown at various pH; spectra were collected at 5 K and harvested at $OD_{600} \approx 0.8$. b.) Bar chart relating the changes in percent effect between NHHS Fe^{III} and nanoparticles of the mutant strain.

EPR Spectra Analysis

The data derived from EPR analysis regarding the WT strain suggests that the steady decrease in NHHS Fe^{III} is, indeed, occuring. Figure 3 below has four EPR traces overlaid and corroborates the MB spectra. As the pH of the growth medium was increased, the signal intensity

in the g = 4.3 region of the spectra, directly relating to NHHS Fe^{III}, decreases. Moreover, the WT strain grown in pH 3 gives the highest signal intensity giving a maximum intensity just over $25x10^{-6}$.

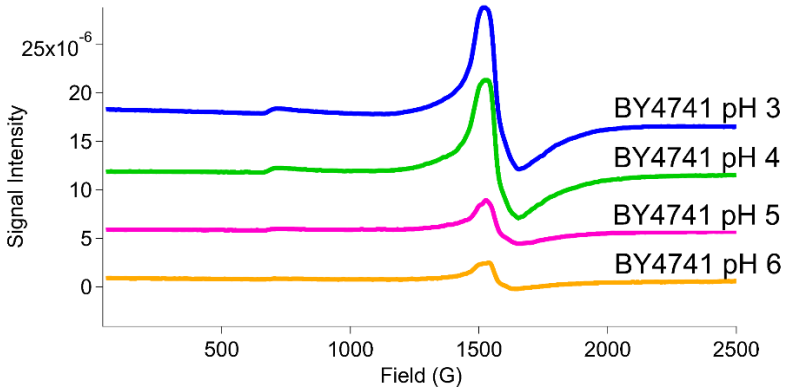

FIGURE 3: BY4741 cells grown at various pH; spectra were collected at 5 K and 30 dB.

When analyzing the mutant EPR trace (Figure 4), it tells a similar story in that the steady decrease in the intensity of the g = 4.3 region of the trace is just as present as it is in the WT. However, there is one major difference between the mutant and the WT and that is the overall signal intensity. As mentioned previously, the WT pH 3 gave a maximum signal intensity of about $25x10^{-6}$ however the ΔVMA2 maximum signal intensity is over $40x10^{-6}$. This pattern of the mutant strain having higher EPR signal intensities than WT continues as the pH increases. This suggests that, in the mutant strain, there is clear Fe regulon dysfunction.

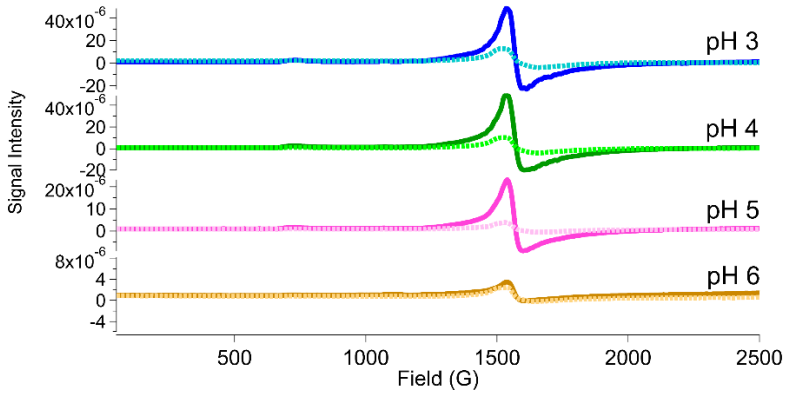

FIGURE 4: The ΔVMA2 strain (solid line) grown at various pH as well as BY4741 (dotted line) grown at corresponding pH; these spectra were all collected at 5 K and 30 dB.

CHAPTER IV

DISCUSSION

WT BY4741 and High pH

Based on the MB spectra of the WT (Figure 1) as pH of the growth medium increases, the total cellular Fe signal seems to decrease. This trend suggests that the WT cell is unable to regulate Fe import as the pH of the growth medium becomes more alkaline. Indeed, this trend was described biochemically via growth studies[10] however biophysical analysis of WT cells grown under these same alkaline conditions has not been conducted until this point. From this study, it is clear that as the growth conditions become more alkaline, cellular Fe transporters, including Fet3 and Atm1, are dysfunctional and, as such, unable to import extracellular Fe. However, the reason for why pH impacts genes of metal ion homeostasis remains unclear.

ΔVMA2 and High pH

Vma2 corresponds to a β subunit of the vacuolar – ATPase which, when knocked out, inactivates the enzyme and results in an alkaline vacuole. Based on a previous *in vitro* study[9], it is expected that as the pH increases, there should be a shift from NHHS Fe^{II} to Fe^{III} nanoparticles. As such, the data from Figure 3 corroborates this notion. There is a clear shift to nanoparticles as the pH was increased incrementally by one pH unit from pH 3 to 7. However, there was also the development of NHHS Fe^{II} signal. The exact location of these species is unknown but we believe this Fe^{II} is building up in concentration the cytosol because of Ccc1's inability to transport Fe into the vacuole. This deficiency is likely due to the degeneration of a proton gradient. However, Mrs3/4, mitochondrial Fe importers, likely remain functional and are

able to import the cytosolic Fe^{II}. However, when vacuolar pH is high it has been shown that the mitochondria is dysfunctional.[11] It is this same dysfunction that we believe explains the dramatic upregulation of the Fe regulon in the Vma2 mutant cells. In a healthy cell, the Fe regulon is ultimately controlled by the activation and deactivation of the Aft1/2 complex. With Fe–S cluster synthesis, the mitochondria release an unknown substrate coined "X-S" which binds to a glutathione-ligated, Fe–S-bridged complex which is transported to the nucleus where it interacts with Fra1/2 to be imported into the nucleus. There, the complex interacts with Aft1/2 to deactivate the Fe regulon and thus cease Fe import into the cell.[12] In the case of the Vma2 mutants, we believe the mitochondria dysfunction is preventing the release of "X–S" and, because of this, the Fe regulon cannot be shut off resulting in the 2-3 fold higher concentration of Fe in the mutant strain. However, this is a working hypothesis and is subject to change based on further Vma2 studies.

Human Relevance

Human cells and yeast cells share many common organelles but the vacuole is not one of them. However, human cells do have a vacuole-like homologue, the lysosome. Like vacuoles, lysosomes bode an acidic environment that is monitored by a V-ATPase that is morphologically similar to that of the vacuole. A recent study has linked lysosomal pH dysregulation to many prominent neurological diseases in humans including both Parkinson's Disease as well as Alzheimer's Disease[13]. Although the work done up to this point has only been foundational, developing an understanding of the mechanisms at work in how pH directly and indirectly affects yeast physiology has the potential to unlock doors to treatment of several diseases that affects tens of millions of people globally.

Future Work

All of the work presented has been completed as a whole cell study. To expand on this project and develop a better understanding of the mechanisms at work, we plan to isolate the cytosol and vacuoles of the WT strain as well as the ΔVMA2 mutant strain. Once isolated, it will be possible to analyze the organelles individually via Mössbauer Spectroscopy as well as LC-ICP-MS. This will enable us to determine whether or not the observed NHHS Fe^{II} is vacuolar or cytosolic. Moreover, the LC-ICP-MS analysis will enable us to determine the molecular mass of the Fe species in each compartment as well as give us accurate concentrations of each species down to nanomolar accuracy.

REFERENCES

(1) Lill, R. *Nature* **2009**, *460* (7257), 831–838.

(2) Dlouhy, A. C.; Outten, C. E. *Met. Ions Life Sci.* **2013**, *12*, 241–278.

(3) Li, L.; Chen, O. S.; Ward, D. M.; Kaplan, J. *J. Biol. Chem.* **2001**, *276* (31), 29515–29519.

(4) Dixon, S. J.; Stockwell, B. R. *Nat. Chem. Biol.* **2014**, *10* (1), 9–17.

(5) Kaplan, C. D.; Kaplan, J. *Chem. Rev.* **2009**, *109* (10), 4536–4552.

(6) Brett, C. L.; Kallay, L.; Hua, Z.; Green, R.; Chyou, A.; Zhang, Y.; Graham, T. R.; Donowitz, M.; Rao, R. *PLoS One* **2011**, *6* (3), 1–9.

(7) Diab, H. I.; Kane, P. M. *J. Biol. Chem.* **2013**, *288* (16), 11366–11377.

(8) Kane, P. M. *J. Bioenerg.* **2007**, *39* (5–6), 415–421.

(9) Cockrell, A. L.; Holmes-Hampton, G. P.; McCormick, S. P.; Chakrabarti, M.; Lindahl, P. A. *Biochemistry* **2011**, *50*, 10275–10283.

(10) Serrano, R.; Bernal, D.; Simón, E.; Ariño, J. *J. Biol. Chem.* **2004**, *279* (19), 19698–19704.

(11) Hughes, A. L.; Gottschling, D. E. *Nature* **2012**, *492* (7428), 261–265.

(12) Outten, C. E.; Albetel, A. N. *Current Opinion in Microbiology*. 2013, pp 662–668.

(13) Colacurcio, D. J.; Nixon, R. A. *Ageing Research Reviews*. 2016, pp 75–88.